Published in final edited form as:
Langmuir. 2010 July 20; 26(14): 12465–12471. doi:10.1021/la101460z.

Dead-end filling of SlipChip evaluated theoretically and experimentally as a function of the surface chemistry and the gap size between the plates for lubricated and dry SlipChips

Liang Li, **Mikhail A. Karymov**, **Kevin P. Nichols**, and **Rustem F. Ismagilov**
Department of Chemistry and Institute for Biophysical Dynamics, The University of Chicago, 929 East 57th, Street, Chicago, IL, 60637

Rustem F. Ismagilov: r-ismagilov@uchicago.edu

Abstract

In this paper, we describe a method to load a microfluidic device, the SlipChip, via dead-end filling. In dead-end filling, the lubricating fluid that fills the SlipChip after assembly is dissipated through the gap between the two plates of the SlipChip instead of flowing through an outlet at the end of the fluidic path. We describe a theoretical model and associated predictions of dead-end filling that takes into consideration the interfacial properties and the gap size between plates of SlipChips. In this method, filling is controlled by the balance of pressures: for filling to occur without leaking, the inlet pressure must be greater than the capillary pressure but less than the maximum sealing pressure. We evaluated our prediction with experiments, and our empirical results agreed well with theory. Internal reservoirs were designed to prevent evaporation during loading of multiple solutions. Solutions were first loaded one at a time into inlet reservoirs; by applying a single pressure source to the device, we were able to fill multiple fluidic paths simultaneously. We used this method to fill both lubricated and dry SlipChips. Dry-loaded SlipChips were fabricated from fluorinated ethylene propylene (FEP) by using hot embossing techniques, and were successfully filled and slipped to perform a simple chemical reaction. The SlipChip design was also modified to enable ease of filling by using multiple access holes to the inlet reservoir.

Introduction

This paper describes a robust method to fill a SlipChip with aqueous solutions, called dead-end filling, that relies on the surface chemistry and gap size of the SlipChip and is applicable to both lubricated and dry SlipChips. SlipChip1⁻6 is an emerging microfluidic platform that enables simple, equipment-free manipulation of large arrays of small fluid volumes. SlipChip is a device made of two plates that move—or slip—relative to one another. Each plate is patterned with arrays of wells and ducts. Various samples and reagents can be manipulated by a program that is encoded into the patterns of wells and ducts. Almost any program can be encoded into the SlipChip, and the program is executed by slipping, which disconnects or connects wells from ducts, and brings complementary wells into fluidic contact or separates them. Applications of SlipChip include protein crystallization,1⁻3 immunoassays,4 and polymerase chain reactions (PCR).5›6 For the SlipChip to function reliably, the reagents or samples must be delivered to individual wells through fluidic paths.

Correspondence to: Rustem F. Ismagilov, r-ismagilov@uchicago.edu.

Supporting Information Available. Additional Experimental Section, tables, and figures and supporting movie. This material is available free of charge via the Internet at http://pubs.acs.org.

An imbalance in pressure could lead to uneven filling in branched paths,7 resulting in unfilled wells towards the end of some paths. To solve the problem of uneven filling, additional long narrow channels were added parallel to the fluidic path to balance pressure.1 Applications performed in SlipChip require quantification, and quantification relies on precise metering of fluid volumes. Fluid volumes are defined by the well size; therefore, complete filling of the wells is essential to the accuracy of metered volumes. In addition, filling of multiple wells in parallel is desirable, to increase the throughput and compatibility with existing automation. Previously, the SlipChip was filled by pipetting the solution into the fluidic path, and allowing the pre-filled lubricating fluid to escape through an outlet.

This paper describes and characterizes, both theoretically and experimentally, an alternative method to fill SlipChips. As the sample solution fills the fluidic path it displaces the lubricating fluid or air that fills the SlipChip after assembly, and instead of allowing the lubricating fluid or air filling the fluidic path to escape through the outlet, the fluid originally in the fluidic path is dissipated through the gap between the plates. We refer to this process “dead-end filling”,8 because the chip design does not contain outlets for each fluidic path. In this method of dead-end filling, all fluidic paths are filled simultaneously by applying a single pressure source.

Experimental Section

Chemicals and Materials

All reagents used in this study were purchased from commercial sources and used without additional purification. Spectrum food dyes were purchased from August Thomsen Corp. (Glen Cove, NY). Fluorocarbon oil FC-40 (a mixture of perfluoro-tri-*n*-butylamine and perfluoro-di-*n*-butylmrthylamine) was obtained from 3M (St. Paul, MN). (Tridecafluoro-1,1,2,2 -tetrahydrooctyl) trichlorosilane (Gelest Inc., Morrisville, PA) was used to silianize and render surfaces fluorophilic. 1H,1H,2H,2H-Perfluoro-1-octanol was obtained from Sigma-Aldrich (St. Louis, MO). Soda-lime glass plates coated with chromium and photoresist were purchased from Telic Company (Valencia, CA). Photomasks were purchased from CAD/Art Services, Inc. (Bandon, OR).

Device fabrication

Glass devices were fabricated by glass etching and sequential silanization to render the surface hydrophobic. Details can be found in the Supporting Information. Plastic devices were fabricated by hot embossing. A glass mold was used to emboss the chip pattern into 1/16” thick fluorinated ethylene propylene (FEP, McMaster-Carr). The chips were embossed at 260 °C, 400 lbs/in2 for 20 minutes in a Carver 3889 hot press. The chips were rapidly cooled to room temperature before pressure was removed. Fabrication of glass molds are detailed in the Supporting Information.

Device assembly

Each device consisted of two plates. Approximately 300 μL of the lubricating fluid (LF) was pipetted onto the bottom plate, and the top plate was slowly placed on top of the bottom plate to avoid trapping air bubbles in channels. The plates, in close contact, were then aligned under a microscope and fixed by 4 paperclips. For the experiments with different gap sizes, beads of 1.5 μm or 3.86 μm in diameter were suspended in LF. These beads were silanized in 5% (v/v) (Tridecafluoro-1,1,2,2-tetrahydrooctyl) trichlorosilane in toluene. The measurement of actual gap size is detailed in the Supporting Information. For experiments with different interfacial tension, 10% (v/v) 1H,1H,2H,2H-Perfluoro-1-octanol (surfactant) was added to LF. Surface tension of aqueous solution in fluorocarbon was measured as

previously reported,9 with modifications described in the Supporting Information. Contact angle and viscosity measurements are also described in the Supporting Information.

Characterizing the physical model SlipChip (Figures 1 and 2)

Inlet pressure control—Inlet pressure was provided by an adjustable N_2 source. The N_2 source was bifurcated into two ends, one of which was connected to a barometer indicating the output pressure in the system and the other was connected to the SlipChip assembly.

Filling solutions—4 μL of a green dye was loaded by pipette on top of the inlets of an assembled device. An O-ring, made from PDMS and ~ 5 mm in height, was then sandwiched between the assembled device and a glass plate and fixed by 4 paperclips. The glass plate bore a nanoport assembly (Upchurch Scientific). The assembly was then connected to the pressure source and solutions were pressurized and forced into the channels in the SlipChip. Any solution leakage was observed in the LF-receiving channel (Figure 2C).

Characterization of filling speed—The channel between two circles was used to characterize the filling speed. Here we used the average volumetric flow rate Q_{ave} to describe the filling speed. The higher the flow rate, the faster the speed. The flow rate is defined as $Q_{ave} = V/t$. V(m)^3 is the volume of the channel to be filled with solution and t (s) is the time recorded to fill the channel. Each experiment was repeated three times.

Filling the lubricated device (Figure 3)

Five solutions were used to fill the FC-lubricated device: a green dye solution was used to fill the fluidic path for the sample; red, blue, orange, and yellow dyes were used to fill the 16 fluidic paths for the reagents. The surface of the plates was patterned with ”micropatterns” (approximately 12.5 μm long, 12.5 μm wide and 2.5 μm deep) with ~ 7.5 μm spacing (see Supporting Information). Such patterns facilitate dissipation of the lubricating FC (Figure S2). To load the sample and multiple reagents simultaneously, the same sample filling procedure that was used to test the physical model was used with the following modifications: all solutions were first loaded into big reservoir wells ahead of the fluidic paths. The filling process was captured using a color digital camera under stereomicroscope Leica MZ16 as a series of sequential images taken with 1 s time intervals (See Movie S1). After filling, the top plate was slipped relative to the bottom plate to bring reagent wells in contact with sample wells and to mix the solutions inside. The slipping process was facilitated by the lubricating FC even though the two plates were clamped by paperclips.

Filling the dry device (Figure 4)

The dead-end filling method was adopted to load a dry FEP SlipChip with aqueous solutions. Following the assembly of the FEP SlipChip in the absence of any lubricating fluid, the SlipChip was sandwiched between two glass slides. The top glass slide had access holes aligned to the inlets of the SlipChip. The “sandwich” was fixed with paper clips. A 1 μL volume of each solution was directly loaded into the inlets using a pipette. The pipette tips were pushed against the inlets through the access holes in the top glass slide. The filling process spontaneously stopped when the solution reached the dead-end. 0.1 M $Fe(NO_3)_3$ was used as a reagent and 0.3 M KSCN was used as a sample. After loading, the top plate of the SlipChip was slipped relative to the bottom plate and solutions were combined while the SlipChip remained sandwiched between the two glass slides throughout the process. The reaction between $Fe(NO_3)_3$ solution and KSCN solution produced a red solution of various complexes including $Fe(SCN)_3$ (Figure 4C).

Filling the multi-access hole storage reservoir in a SlipChip (Figure 5)

1.5 μL solution of a green food dye was loaded into the reservoir via the inlet, for less than one second. 8 kPa of pressure was then applied to both inlet and outlet of the reservoir for less than one minute to drive the solution from the reservoir to the filling channel (Figure 5C–D).

Results and discussion

Physical model

To predict the process of dead-end filling, we developed a physical model (Figure 1). In this model, we investigated dead-end filling of phase 1 in a single channel to replace a pre-filled phase 2. Phase 1 and phase 2 are immiscible, and the contact angle of phase 1 on the channel surface in the presence of phase 2 is larger than 90°; i.e. phase 1 is the non-wetting fluid and phase 2 is the wetting fluid. Dead-end filling could be described as follows: the non-wetting fluid (phase 1) is placed at the inlet. Applied pressure drives the fluid into the fluidic path connected to the inlet, pushing out an immiscible wetting fluid (phase 2). Phase 2 is dissipated out through the gap (Figure 1C). Phase 1 stops flowing when it reaches the dead end.

Characterization of the physical model

To characterize the physical model experimentally, we fabricated a simplified model SlipChip (Figure 1). We designated a stained aqueous solution to be phase 1 and a lubricating fluid (LF) to be phase 2. The surface of the model SlipChip was modified to be preferentially wetted by LF. Using the model SlipChip, we aimed to 1) recognize the pressure range where robust filling can be achieved without leaking; and 2) determine parameters that affect filling speed.

Inlet pressure has to be higher than capillary pressure—Since the surface of the chip is wetted by LF (phase 2), the aqueous solution could not be loaded by capillary flow. Instead, the pressure applied at the inlet (ΔP_{inlet}, Pa) has to overcome a resistant pressure, the capillary pressure (ΔP_{cap} , Pa) at the interface between the aqueous and LF (Figure 1B).

An increase in the cross-sectional dimension of the channel decreases the resistant capillary pressure ΔP_{cap} (Pa, Equation 1), and consequently facilitates filling. In Equation 1, γ (N/m) is the surface tension, R_w ($R_w = w/2\cos\theta$, m) and R_h ($R_h = h/2\cos\theta$, m) are the interface approximate curvatures in the horizontal (width w, m) and vertical (height h, m) directions; θ (°) is a contact angle. Generally it is difficult to determine the precise shape of the interface even in rectangular channels,[10,11] especially if this interface is formed partially by the solid surface and partially by the liquid-liquid interface, as in this case. According to the Young-Laplace equation, the approximate pressure difference at the interface between the aqueous and LF phases is expressed in Equation 1. In the simple model SlipChip, we designed an inlet channel (Figure 1A) to be equal or smaller in size than the main filling channel. The presence of aqueous solution in the inlet reservoir at a certain inlet pressure guarantees that the pressure is high enough for filling of the main filling channel.

$$\Delta P_{cap} = -\gamma\,(1/R_w + 1/R_h) = -2\gamma\left(\frac{1}{w}+\frac{1}{h}\right)\cos\theta \qquad \text{Equation 1}$$

The sealing pressure prevents the aqueous phase from leaking out of the filling channel—In a SlipChip, a gap exists between the two plates and the aqueous

solution can leak out of the filling channel (Figure 1E, cross-sectional view). The sealing pressure, P_{seal} (Pa) (Equation 2) prevents leakage.

$$P_{seal} = -2 \times \gamma \times \cos\theta / d \quad \text{Equation 2}$$

Here, γ (N/m) is the surface tension between the aqueous phase and LF; θ(°) is the contact angle between the aqueous phase and surface of the SlipChip in LF; d (m) is the gap distance between the two plates of the SlipChip. The inlet pressure must be smaller than the sealing pressure (Equation 3) to avoid leakage into the gap; if the inlet pressure is higher, the aqueous phase will flow between the plates, causing leaking.

$$\Delta P_{inlet} < P_{seal} \quad \text{Equation 3}$$

We tested the prediction in the model SlipChip (Figure 2). This simple model SlipChip contained multiple filling channels with increasing size of the channel cross section. Each channel was formed by overlapping two ducts, one in the top plate and another in the bottom plate, creating a symmetrical channel (Figure 1C, E). The channel bore two circular reservoirs, one at the inlet and one as the dead end. The inlet reservoir served as a buffer region to slow the flow, therefore allowing us to better determine the start of filling. The dead-end reservoir helped visualize the end point of filling. We also designed receiving channels alongside the filling channels to receive dissipated phase 2 (LF). Those receiving channels were open to ambient pressure and they were wide enough to assume that the pressure inside the receiving channels were uniform. The receiving channels also helped visualization of leakage because any leakage of phase 1 from the filling channel would accumulate in the receiving channel (Figure 1D, E and Figure 2C). We measured the static contact angles of the stained aqueous solutions on the SlipChip plate in the presence of LF; however, such contact angles could be different from those within the device (Figure 1C), especially under flow conditions. Therefore, to characterize the performance of the model SlipChip, we used the maximal sealing pressure, $P_{seal,max}$ (Pa), assuming $\theta = 180°$ as the upper limit of the allowed inlet pressure (Equation 4). To vary the value of the upper limit, we changed the maximum sealing pressure by varying the interfacial tension (γ) and the gap between plates, by adding fluorinated surfactants and monodispersed glass beads in LF respectively. In accordance with our prediction, leaking depended on inlet pressure and not on channel size (Figure 2). That is, when the inlet pressure was lower than the maximum sealing pressure, all channels were filled without leaking (Figure 2B); and when the inlet pressure was higher than the maximum pressure, leaking occurred in all channels (Figure 2C).

$$\Delta P_{inlet} < P_{seal,\max} = 2\gamma / d \quad \text{Equation 4}$$

Dissipation of LF limits the filling speed—The equations predicted that changing related parameters affects filling speed while changing unrelated parameters does not. In the simple model SlipChip, ΔP_{flow} (Pa) is the pressure difference between the opposite ends of the channel filled with aqueous phase 1 (Equation 5) and it includes three terms (Equation 6): ΔP_1 (Pa), the pressure difference due to flow resistance of the aqueous phase (phase 1) in the filling channel; ΔP_2 (Pa), the pressure difference due to flow resistance of LF (phase 2) in the filling channel; and ΔP_3 (Pa), the pressure difference due to flow resistance of LF between the two plates of a SlipChip. Equation 7, obtained by combining Equation 5 and

Equation 6, expresses the pressure difference along the system. The pressure difference due to flow resistance is expressed in Equation 8,12 where μ_i (Pa×s) is the viscosity of the corresponding fluid *i* (μ_i is the viscosity of the aqueous phase, μ_2 and μ_3 are the same, the viscosity of the lubricating phase) and L_i (m) is the average length of the fluid path. Q_i (m^3/s) is the flow rate of discharge. Due to conservation of mass, Q_1, Q_2, and Q_3 are the same. h_i is the height of the fluidic path; therefore, h_1 and h_2 are the same and equal to the height of the channel. h_3 is the gap between the two plates of the SlipChip. w_i (m) is the width of the fluidic path. w_1 and w_2 are the same, equal to the width of the filling channel. In principle, Equation 8 predicts the flow rate (Q), which describes the filling speed.

$$\Delta P_{flow}=\Delta P_{inlet}-\Delta P_{cap} \quad \text{Equation 5}$$

$$\Delta P_{flow}=\Delta P_1+\Delta P_2+\Delta P_3 \quad \text{Equation 6}$$

$$\Delta P_{inlet}=\Delta P_1+\Delta P_2+\Delta P_3+\Delta P_{cap} \quad \text{Equation 7}$$

$$\Delta P_i=\frac{\pi^4\mu_i L_i Q_i}{8{h_i}^3 w_i\left(1-\frac{2h_i}{\pi w_i}\tanh\left(\frac{\pi w_i}{2h_i}\right)\right)} \quad \text{Equation 8}$$

We characterized the filling speed in the model SlipChip. We assumed that L_1 and L_2 were the same, equal to half the length of the whole filling channel, and L_3 was the distance between the filling channel and the large receiving channel. We assumed w_3 was half the length of the filling channel. In the model SlipChip, the hyperbolic tangent asymptotically went to 1 as the channel aspect ratio increased (height decreases and/or width of the channel increases); and the pressure drop ΔP_i in the channel changed proportionally to ($1/{h_i}^3 w_i$). ΔP_3 was much larger than ΔP_1 or ΔP_2 because $h_3 \ll h_1 = h_2 < w_i$. In our experiments, ΔP_{inlet} was always much larger than ΔP_{cap} in order to fill the channel (Equation 5). Therefore, ΔP_{inlet} was approximately the same as ΔP_3. (Equation 9). By combining Equations 8 and 9 with the assumption that the hyperbolic tangent ~ 1, we obtained Equation 10, which indicated that the filling rate of the aqueous solution, at a fixed inlet pressure, was determined by the rate of dissipation of the lubricating fluid, which in turn, was determined by its viscosity and the gap size.

$$\Delta P_{inlet} \approx \Delta P_3 \quad \text{Equation 9}$$

$$Q=Q_3=\frac{8{h_3}^3 \times w_3 \times \Delta P_{inlet}}{\pi^4 \mu_3 \times L_3} \quad \text{Equation 10}$$

We experimentally tested our prediction by varying h_3 and μ_3 while keeping w_3, L_3, and ΔP_{inlet} constant at 1×10^4 μm, 2×10^3 μm and 5.3×10^3 Pa respectively. We used beads of defined sizes to control the gap (see Experimental Section in Supporting Information). We confirmed qualitatively that the filling rate was sensitive to ${h_3}^3$ and μ_3 (Table 1, n = 3 for all

experiments) and not sensitive to change of other parameters related to ΔP_1, ΔP_2 and ΔP_{cap} (Table 2, n=3 for all experiments).

Filling a more complex SlipChip by dead-end filling

We used the physical model and designed a system to use dead-end filling to fill SlipChips with multiple solutions at the same time (Figure 3). We used a previously reported design, similar to the user-loaded SlipChip screening conditions for protein crystallization with 16 different precipitants and 11 mixing ratios for each precipitant.2 We made the following modifications to simplify the design: straight ducts were fabricated without turns, and no narrow channels were used to balance the pressure. In addition, we added an inlet reservoir for each solution. The inlet reservoir was designed not only to buffer the flow as described for the simple model SlipChip, but also for storage and to prevent evaporation. Solutions were first loaded into the inlet reservoirs (Figure 3C), before applying pressure to fill the fluidic paths (Figure 3D–F). We also designed smaller outlet reservoirs to prevent undesirable back flow. To minimize the flow pressure generated by dissipation of lubricating fluid between plates while maintaining the same sealing pressure, receiving channels were fabricated near the fluidic path so that the flowing distance of the lubricating fluid was minimized. We made small patterns (~ 2.5 μm in depth) on the contacting surface of the SlipChip to further lower the flow pressure between plates (See Experimental Section and Figure S2 in the Supporting Information). The similarity between this chip and the user-loaded SlipChip2 make applications to crystallization straightforward. This SlipChip design can also perform multiplexed screening of crystallization conditions by loading multiple reagents at multiple mixing ratios. Loading reagents at multiple mixing ratios allows for on-chip titrations. The ability to titrate a reagent on-chip is important for protein crystallization, as the concentration of a reagent, in addition to its identity, can affect the outcome of crystallization.2

Filling of the reagent wells spontaneously ceased when the solution reached the end of the fluidic path even though the sample fluidic path with more wells were still being filled (see Supporting Movie S1, details of the movie are in the Supporting Information). As a result, all the solutions can be loaded using a single pressure source.

Filling a dry device by dead-end filling

We wished to test whether the same approaches would work for a dry SlipChip, in which no liquid is used to lubricate the plates. While lubricated SlipChips prevent evaporation from wells and eliminate the air/water interface that is undesirable in some applications, dry SlipChips could be attractive for applications where the lubricating fluids are not compatible. In addition, we predicted that filling would be rapid because air has low viscosity and can escape rapidly between the plates. The design of the device was the same as the device shown in Figure 3, but this device was made from plastics by hot embossing FEP using glass molds (see Figure S1 and Experimental Section in Supporting Information). The plastic SlipChip was sandwiched between two glass plates and loaded in the absence of any lubricating fluid. A simple chemical reaction was used to demonstrate this dry-loading (Figure 4). Using this method, the solutions filled the fluidic paths of the SlipChip completely (Figure 4B), and slipping successfully combined the reagent and sample to perform the reaction between the $Fe(NO_3)_3$ solution (reagent) and the KSCN solution (sample) (Figure 4C). This reaction produced a red solution of various complexes, including $Fe(SCN)_3$. No evidence of cross-contamination was seen, and no red complex formed in the ducts.

Designing a SlipChip to simplify loading and allowing for stable storage of solutions

We also developed a method to easily load solution into a storage reservoir prior to dead-end filling (Figure 5). Loading of the solution into the reservoir as shown in Figure 3 requires drainage of the lubricating fluid through the gap, and in some designs, this drainage may become rate limiting, especially where dense arrays are loaded and lubricating fluid from multiple reservoirs drains through the same paths. To eliminate this potential problem, and to enable robust loading by a wide range of equipment independently of the design of the chip and the density of the reservoirs, we tested an additional simple idea for creating a storage reservoir between the two plates into which a solution can be very rapidly loaded (Figure 5A, B). In this design, each reservoir has an inlet and an outlet, creating a very low resistance fluidic path for loading. The shape of the reservoir is such that surface tension would drive the loaded solution into the center of the storage reservoir (Figure 5C), where it would come into contact with the filling channel. Dead end filling would occur when pressure is applied to both the inlet and outlet of the storage reservoir (Figure 5D). The solution, prior to filling, remains surrounded by the lubricating fluid, allowing for stable storage and preventing evaporation. We found that this idea is sound (Figure 5), and we recommend that it be incorporated into future designs of dead-end loaded SlipChips.

Conclusions

This paper presents ideas, theory, and experiments for a method of loading SlipChips via dead-end filling. We validated this method to fill both lubricated (with fluorocarbons as lubricating fluids) and dry (with air between the plates) SlipChips with aqueous solutions. This method can be used to make a SlipChip with inlets compatible with the SBS (Society for Biomolecular Science) standard format, such as 96, 384, or 1536 well plates, or using such a plate as one of the plates of the SlipChip. Standard equipment, such as pipettors or robotics, can be used to load the solutions into the plate; after pressurization, desired volumes would be formed inside the SlipChip. In addition, a reservoir to store solutions at the inlets can help prevent evaporation, a common problem for small-volume dispensing. This method can be directly extended to protein crystallization,13 and would be useful for performing immunoassays and PCR reactions. This paper provides a simple method to control fluid flow in a microfluidic device to complement other creative ways in which flow has been generated and controlled,14–19 and SlipChip may find similar applications. The concept of draining a fluid through a gap between plates can be extended to other applications such as the separation of two phases. For example, very small scale liquid-liquid separations20 could be accomplished by directing one phase to the gap while leaving another phase within the channel. In addition, using capillary pressure to restrict fluidic flow and its application in dead-end filling could also be extended to sealed devices if narrow channels with high capillary pressure are used. A similar system21 has been described to facilitate merging of two sequential droplets. In this paper, we used aqueous solution as non-wetting phase 1; however, by modifying the surface of the SlipChip to be hydrophilic, this system could be extended to other systems where phase 1 is oil-based and phase 2 is aqueous.

The “dry SlipChip” described here, operating without a lubricating liquid, should be useful to further simplify operation of the SlipChip. When aqueous solutions are used, the dry SlipChip benefits from superhydrophobic surfaces with high contact angle of the aqueous phase and low contact angle hysteresis. Such surfaces can be achieved by a number of approaches, including the use of nanoporous and microporous polymers,22,23 phase separation of block copolymers,24 surface coatings,25 surface roughness,26,27 and a number of other approaches.28–32 We believe that the dead-end filling and dry SlipChip will play a role in a broad range of applications, including enabling diagnostics in resource-limited settings.

Supplementary Material

Refer to Web version on PubMed Central for supplementary material.

Acknowledgments

This work was supported by the NIH Protein Structure Initiative Specialized Centers Grant GM074961 (ATCG3D) and the NIH Director's Pioneer Award Program, part of the NIH Roadmap for Medical Research (1 DP1 OD003584). Part of this work was performed at the Materials Research Science and Engineering Centers microfluidic facility (funded by the National Science Foundation). We thank Heidi Park for contributions to writing and editing this manuscript.

References

1. Du W, Li L, Nichols KN, Ismagilov RF. Lab Chip. 2009; 9:2286–2292. [PubMed: 19636458]
2. Li L, Du W, Ismagilov RF. J Am Chem Soc. 2010; 132:106–111. [PubMed: 20000708]
3. Li L, Du W, Ismagilov RF. J Am Chem Soc. 2010; 132:112–119. [PubMed: 20000709]
4. Liu W, Chen D, Du W, Nichols KP, Ismagilov RF. Anal Chem. 2010; 82:3276–3282. [PubMed: 20334360]
5. Shen F, Du W, Davydova E, Karymov M, Pandey J, Ismagilov RF. Anal Chem. 2010; 82:4606–4612. [PubMed: 20446698]
6. Shen F, Du W, Kreutz JE, Fok A, Ismagilov RF. Lab Chip. 201010.1039/C004521G
7. Adamson DN, Mustafi D, Zhang JX, Zheng B, Ismagilov RF. Lab Chip. 2006; 6:1178–1186. [PubMed: 16929397]
8. Hansen CL, Skordalakes E, Berger JM, Quake SR. Proc Natl Acad Sci U S A. 2002; 99:16531–16536. [PubMed: 12486223]
9. Roach LS, Song H, Ismagilov RF. Anal Chem. 2005; 77:785–796. [PubMed: 15679345]
10. Ajaev VS, Homsy GM. J Colloid Interf Sci. 2001; 244:180–189.
11. Ajaev VS, Homsy GM. J Colloid Interf Sci. 2001; 240:259–271.
12. Ichikawa N, Hosokawa K, Maeda R. J Colloid Interf Sci. 2004; 280:155–164.
13. Li L, Ismagilov RF. Ann Rev Biophys. 2010; 39:139–158. [PubMed: 20192773]
14. Walker GM, Beebe DJ. Lab Chip. 2002; 2:131–134. [PubMed: 15100822]
15. Cho BS, Schuster TG, Zhu XY, Chang D, Smith GD, Takayama S. Anal Chem. 2003; 75:1671–1675. [PubMed: 12705601]
16. Clicq D, Vervoort N, Vounckx R, Ottevaere H, Buijs J, Gooijer C, Ariese F, Baron GV, Desmet G. J Chromatogr A. 2002; 979:33–42. [PubMed: 12498231]
17. Tokeshi, M.; Kitamori, T. Advances in Flow Analysis. Trojanowicz, M., editor. Wiley-VCH; Weinheim: 2008. p. 149-166.
18. Kuwata, M.; Kitamori, T. microTAS. Tokyo, Japan: 2006. p. 1130-1132.
19. Chan WK, Yang C. J Micromech Microeng. 2005; 15:1722–1728.
20. Kralj JG, Sahoo HR, Jensen KF. Lab Chip. 2007; 7:256–263. [PubMed: 17268629]
21. Niu X, Gulati S, Edel JB, deMello AJ. Lab Chip. 2008; 8:1837–1841. [PubMed: 18941682]
22. Jiang L, Zhao Y, Zhai J. Angew Chem-Int Edit. 2004; 43:4338–4341.
23. Erbil HY, Demirel AL, Avci Y, Mert O. Science. 2003; 299:1377–1380. [PubMed: 12610300]
24. Levkin PA, Svec F, Frechet JMJ. Adv Funct Mater. 2009; 19:1993–1998. [PubMed: 20160978]
25. Coulson SR, Woodward IS, Badyal JPS, Brewer SA, Willis C. Chem Mat. 2000; 12:2031–2038.
26. Cortese B, D'Amone S, Manca M, Viola I, Cingolani R, Gigli G. Langmuir. 2008; 24:2712–2718. [PubMed: 18217778]
27. Miwa M, Nakajima A, Fujishima A, Hashimoto K, Watanabe T. Langmuir. 2000; 16:5754–5760.
28. Li XM, He T, Crego-Calama M, Reinhoudt DN. Langmuir. 2008; 24:8008–8012. [PubMed: 18605708]

29. Jin MH, Feng XJ, Xi JM, Zhai J, Cho KW, Feng L, Jiang L. Macromol Rapid Commun. 2005; 26:1805–1809.
30. Martines E, Seunarine K, Morgan H, Gadegaard N, Wilkinson CDW, Riehle MO. Nano Lett. 2005; 5:2097–2103. [PubMed: 16218745]
31. Patankar NA. Langmuir. 2004; 20:8209–8213. [PubMed: 15350093]
32. Morra M, Occhiello E, Garbassi F. Langmuir. 1989; 5:872–876.

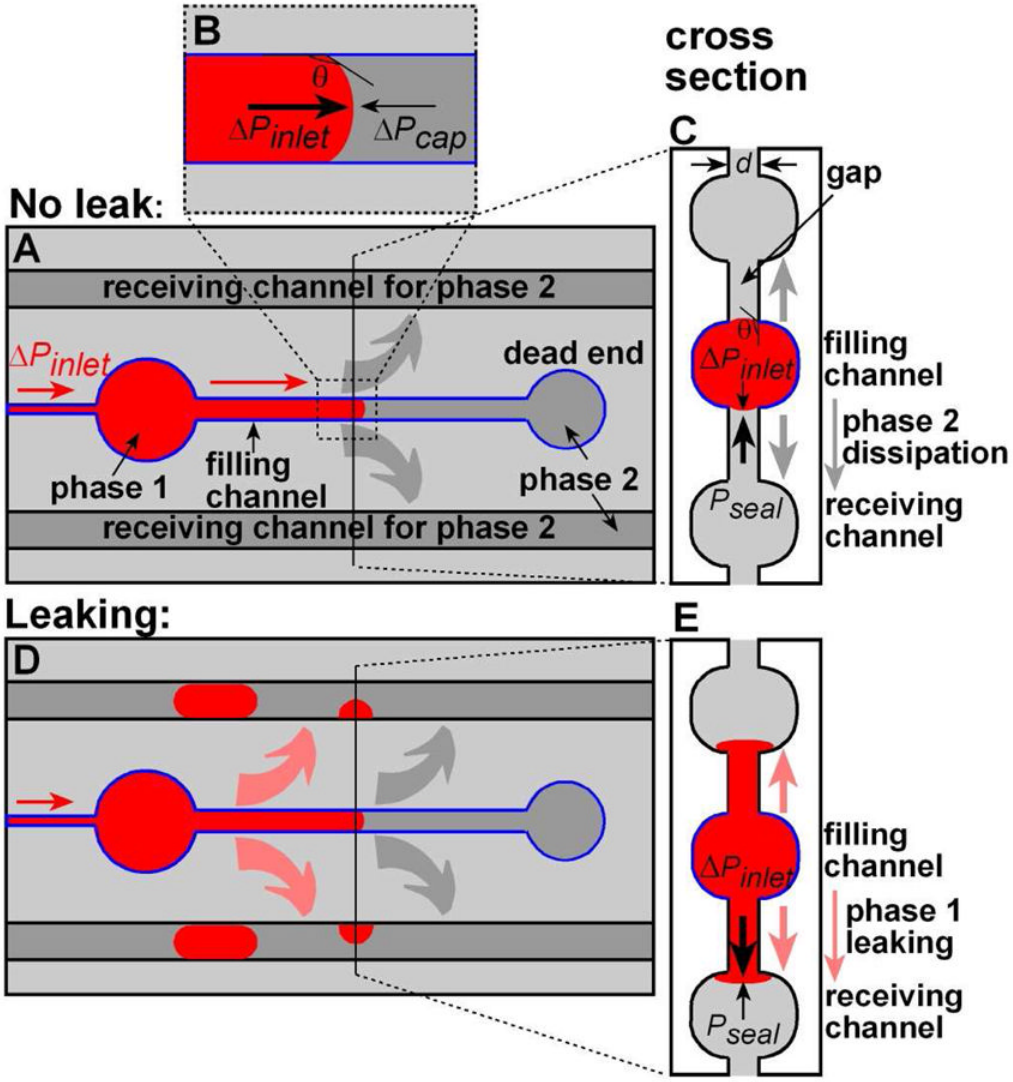

Figure 1.

The model SlipChip used to test the physical model that describes the process of dead-end filling. (A) A top view of the SlipChip with no leaking, showing that Phase 1 (red) was filled (red arrows) in a filling channel (outlined in blue) without an outlet, pushing out phase 2 (grey), which flowed (grey arrows) into the surrounding receiving channels through the gap. (B) A zoom-in top view of the interface between phase 1 and phase 2 in the filling channel. ΔP_{inlet} (indicated by a thick arrow) > ΔP_{cap} ensures filling of the channel. (C) A cross section of the SlipChip when in the regime of no leak (see Figure 2B). P_{seal} (indicated by a thick black arrow) > ΔP_{inlet} confines phase 1 in the filling channel. Phase 2 is dissipated through the gap between the plates to the receiving channel. (D) A top view of the SlipChip when leaking occurred, showing that Phase 1 (red) was filled in a filling channel and also leaked (indicated by pink arrows) into surrounding receiving channels. (E) A cross section of the SlipChip when in the regime of leaking (see Figure 2C). ΔP_{inlet} (indicated by a thick arrow) > P_{seal} pushes phase 1 through the gap into the receiving channel, causing leaking. Parameters are described in Equations 1–3.

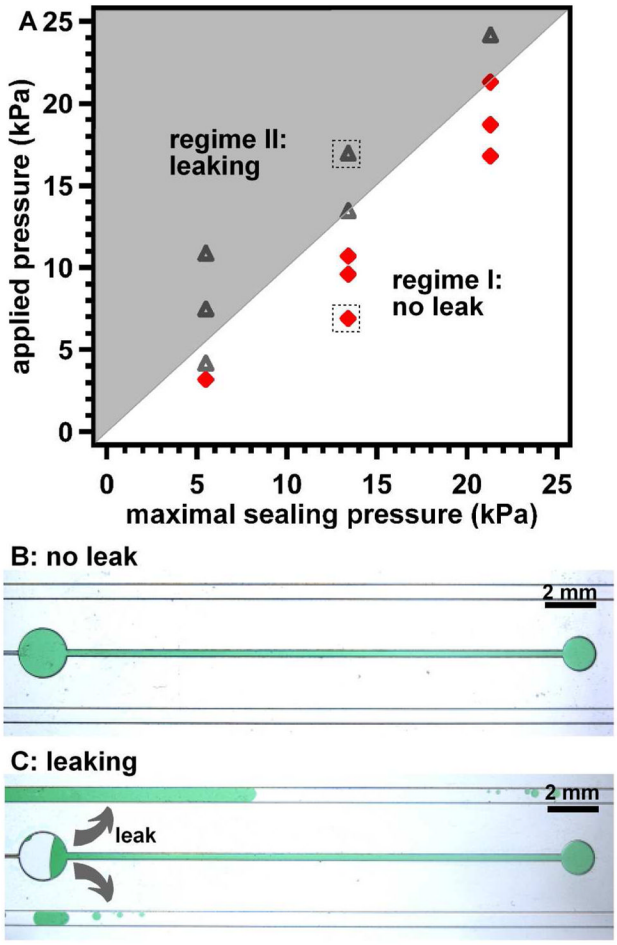

Figure 2.

Regimes of no leak (regime I) and leaking (regime II) as a function of both the applied pressure and the maximum sealing pressure. (A) An experimental phase diagram indicates the regimes of no leak (I) and leaking (II). Each point on the phase diagram represents one experiment. Diamonds (♦) represent experiments where no leakage occurred, and triangles (△) represent experiments where leakage occurred. The white area in the phase diagram indicates regime I (predicting no leak) and the shaded area indicates regime II (predicting leaking). The two areas were separated at the highest predicted pressures that did not induce leaking. (B) A microphotograph of no leakage corresponds to the diamond surrounded by a dashed square in (A). (C) A microphotograph of leaking corresponds to the triangle surrounded by a dashed square in (A).

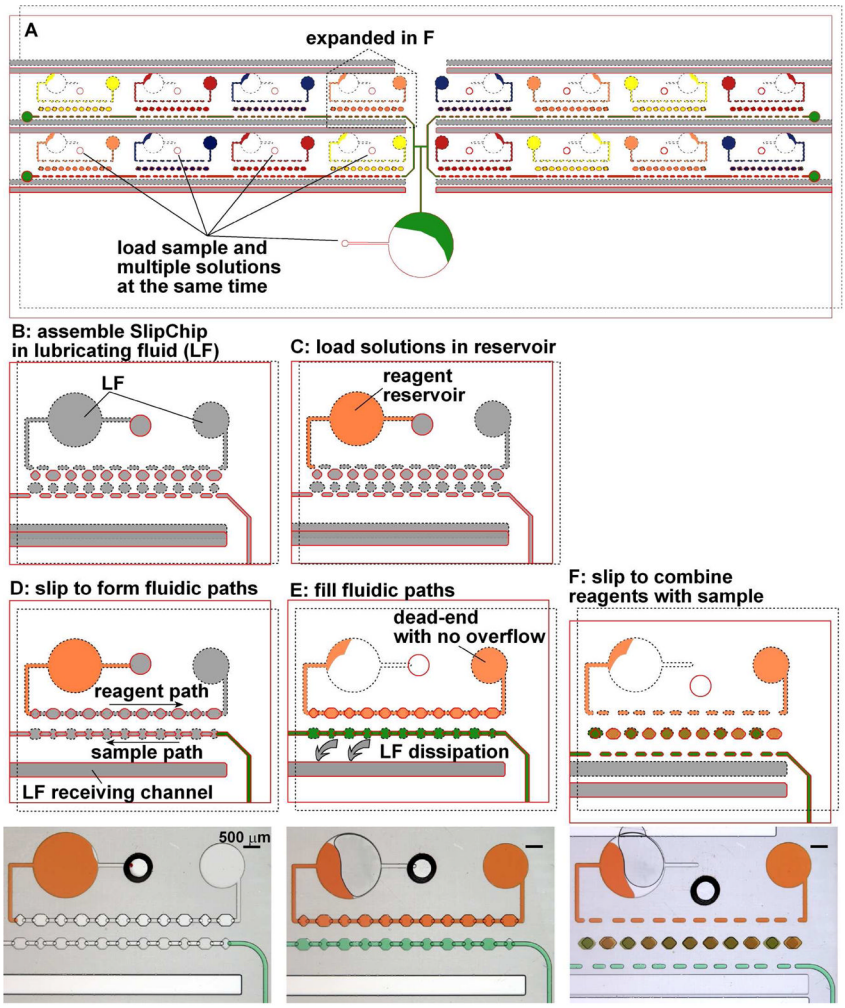

Figure 3.

Successful loading of a SlipChip via dead-end filling. Green color represents the sample, and pink, yellow, orange, and blue colors represent the reagents. Although the sample path and reagent paths were filled at slightly different rates (see Supporting Movie S1), all wells were filled completely (as shown in the zoom-in on green and orange wells). Features in the top plate are outlined in solid red lines, features in the bottom plate are outlined in dashed black lines. Grey colored wells are filled with the lubricating fluid (LF). A) Schematic of the entire SlipChip. The spacing of the inlets for reagents was designed to be compatible with an eight-channel pipetter. The wide horizontal channels are LF receiving channels. B) SlipChip was assembled under the lubricating fluid. C) The reagent reservoir was loaded with solution. All reagent reservoirs and the sample reservoir were loaded before filling any fluidic paths. D) The SlipChip was slipped to form 17 separate fluidic paths in the SlipChip. E) By applying pressure, the wells in the SlipChip were filled via dead-end filling. LF was dissipated through the receiving channels. F) The SlipChip was slipped again to combine reagents with the sample. In D–F, the microphotograph below the schematic shows a food dye experiment in the dead-end filled SlipChip. The contacting surface of the two plates of the SlipChip was micropatterned to facilitate LF dissipation.

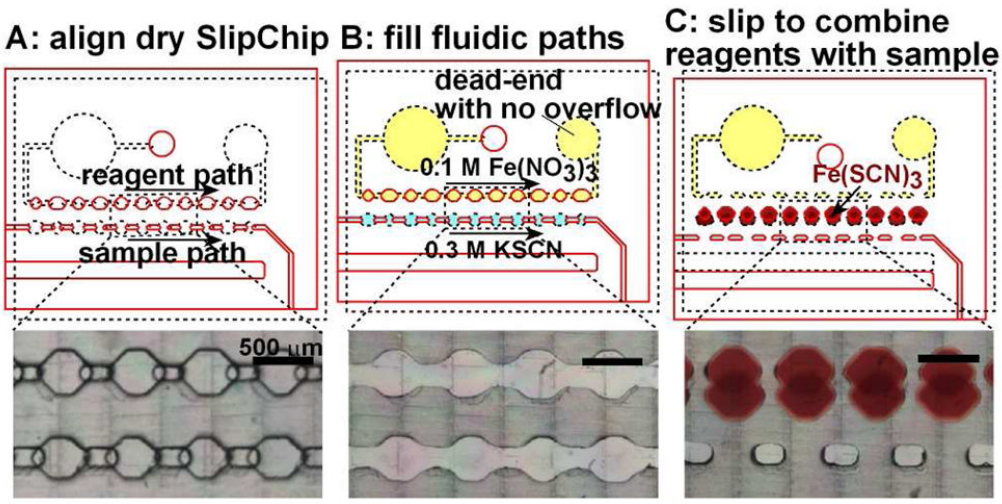

Figure 4.

Performing a simple chemical reaction in a dry-loaded FEP device. Schematics show features in the top plate (outlined in red) and features in the bottom plate (outlined in dashed black lines). Microphotographs show the wells and ducts in the SlipChip. A) The two plates of the SlipChip were aligned in the absence of lubricating fluid to form the fluidic paths for the reagent and the sample. B) The reagent and sample solutions were loaded into the SlipChip via dead-end filling. C) The SlipChip was slipped to combine the reagents with the sample. The reaction was accompanied by the color change from clear to red.

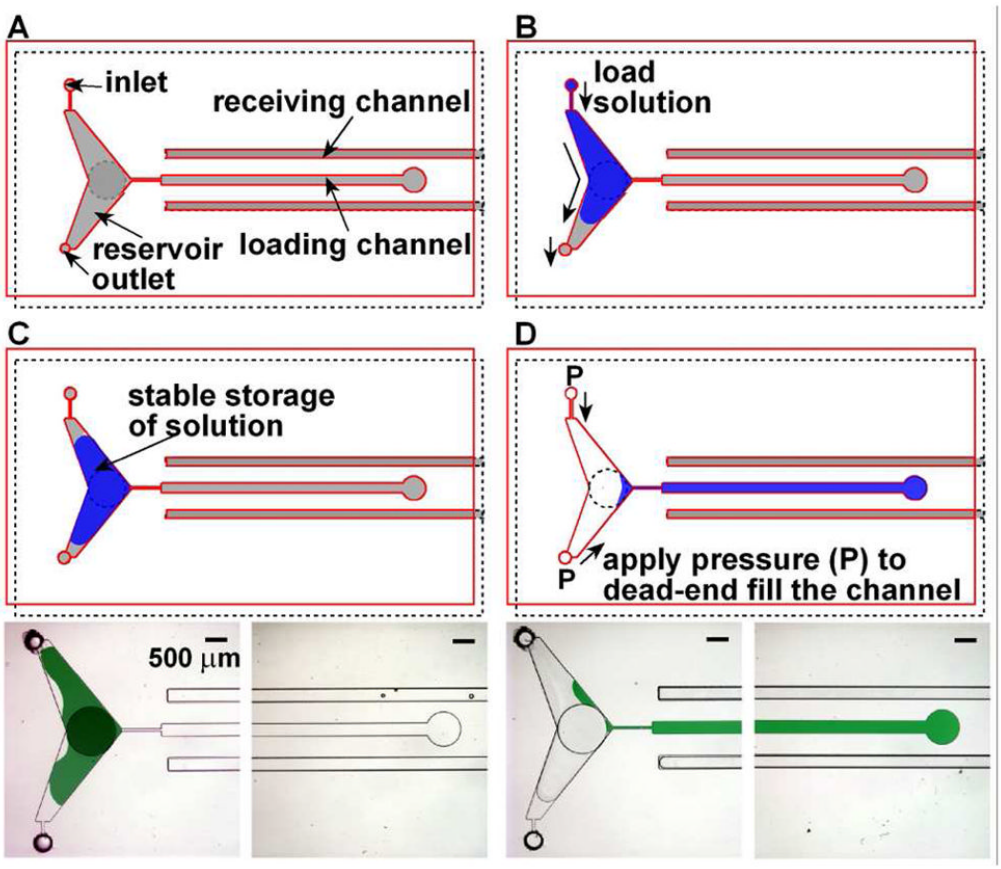

Figure 5.

A design to enable rapid loading of solutions into SlipChip and stable storage. A) The device contains two access holes (an inlet and an outlet) connected to a reservoir for solution storage in one plate and a well of comparable size in the other plate to expand the storage volume. B) When loading a solution into the reservoir through the inlet, lubricant escapes through the outlet with minimum pressure resistance. C) The loaded solution, surrounded by lubricant, is stored in the reservoir without evaporation. Below are two microphotographs, one of the reservoir (left), another of the dead end (right), to show stable storage of a solution of green dye in the reservoir. D) Applying pressure through both the inlet and the outlet drives the stored solution into the filling channel with the lubricant escaping into the receiving channels. Below are two microphotographs at the same locations as in C), to show the channel being filled with the solution by dead-end filling.

Table 1

Effects of SlipChip gap and viscosity of lubricating fluid on filling rates.

Exp. No.	μ_3 (mPa×s)	h_3 (μm)	Q (nL/s) w_1=w_2=141 μm	Q (nL/s) w_1=w_2=562 μm	predicted Q (nL/s)
1	3.4	1.9	4.6±0.3	5.4±0.3	4.4
2	3.4	4.6	40±6	52±3	62
3	1.4	1.9	12±2	16±1	11

Table 2

Viscosity of phase 1, surface tension between phase 1 and phase 2, and the size of the filling channel did not affect loading rate.

Exp. No.	μ_1 (mPa×s)	μ_2, μ_3 (mPa×s)	γ(mN/m)	$h_3(\mu m)$	Q (nL/s) $w_1 = w_2 = 141$ μm	Q (nL/s) $w_1 = w_2 = 562$ μm	predicted Q (nL/s)
1	1.0	3.4	49.0	1.9	4.6±0.3	5.4±0.3	4.4
2	1.0	3.4	12.7	1.9	6.1±0.5	6.4±1.2	4.4
3	3.3	3.4	36.7	1.9	5.0±0.3	5.4±0.6	4.4

Langmuir. Author manuscript; available in PMC 2011 July 20.